Proceedings of the ASME 2020 International Design Engineering Technical Conferences & Computers and Information in Engineering Conference
IDETC/CIE 2020
August 16-19, 2020, St. Louis, MO, USA

IDETC2020-22600

KINEMATIC ANALYSIS OF A 5-DOF POSITIONER FOR PRECISION ADDITIVE MANUFACTURING

Mohammad Hossein Saadatzi*, **Dan O. Popa**
Next Generation Systems Research Group
Dept. of Electrical and Computer Eng.
University of Louisville
Louisville, Kentucky 40208
Email: [mh.saadatzi,dan.popa]@louisville.edu

ABSTRACT

Additive manufacturing, as a viable industrial-production technology, requires multi-DOF positioning with high precision and repeatability for either the printer head, or the part being printed. In this paper we present a novel methodology to analyze the error propagation informing the design of a high-precision robotic 5-DOF positioner for applications in additive manufacturing. We designed our positioner through serial attachment of linear and rotational stages by comparing the precision of three different kinematic arrangements of stages. Within order to minimize positioning errors in Cartesian space, the kinematic sensitivity of the mechanisms end-effector relative to the maximum expected error of each joint was computed, and the kinematic configuration with smallest 6D positioning error at the end-effector was selected. The methodology employed in this paper for the error propagation analysis of serial kinematic chains has a great level of generality and can facilitate the design and optimization of a wide-class of multi-DOF positioners.

NOMENCLATURE

l_1 The distance from the top of the table to the center of the tilt stage. l_1 is 45cm here.
l_2 The distance from the center of the tilt stage to the center of the end-effector (on its top). l_2 is 6cm here.
d_X, d_x, d_y, d_z Variables of the linear stages.
θ_t, θ_z Variables of the rotational stages.
σ_r, σ_p Maximum end-effector rotation, and point-displacement.
P, R Linear (prismatic) and Rotational (revolute) stages.
q_i, x_j Joint space and Cartesian space variables.
J_v, J_ω Translational and rotational partitions of the Jacobian.

INTRODUCTION

Additive manufacturing for generation of 3D parts often requires positioners for either the printer head, or for the platform on which the part is built. Typical 3-DOF positioners used by industrial 3D printers offer precisions above 10 microns, including Hyrel3D® (with precision of at least 10 microns along each axis), and MakerGear® platforms (with minimum precision of 20 microns). There have also been some development of high precision positioners for microrobotic and microassembly applications [1–3]. However, they are typically not designed in the same kinematic configuration as used in typical 3D printers.

This paper is devoted to the kinematic design of a novel 5-axis micro-positioner to be used in conjunction with a high precision Aerosol Jetting printer [4]. The positioner is part of the Nexus system, a novel multi-robot and multi-process instrument being designed and built in support of the US scientific community. The positioner with maximum height of 50cm is supposed to carry a payload of 2kg. The Nexus has microassembly,

*Address all correspondence to this author.

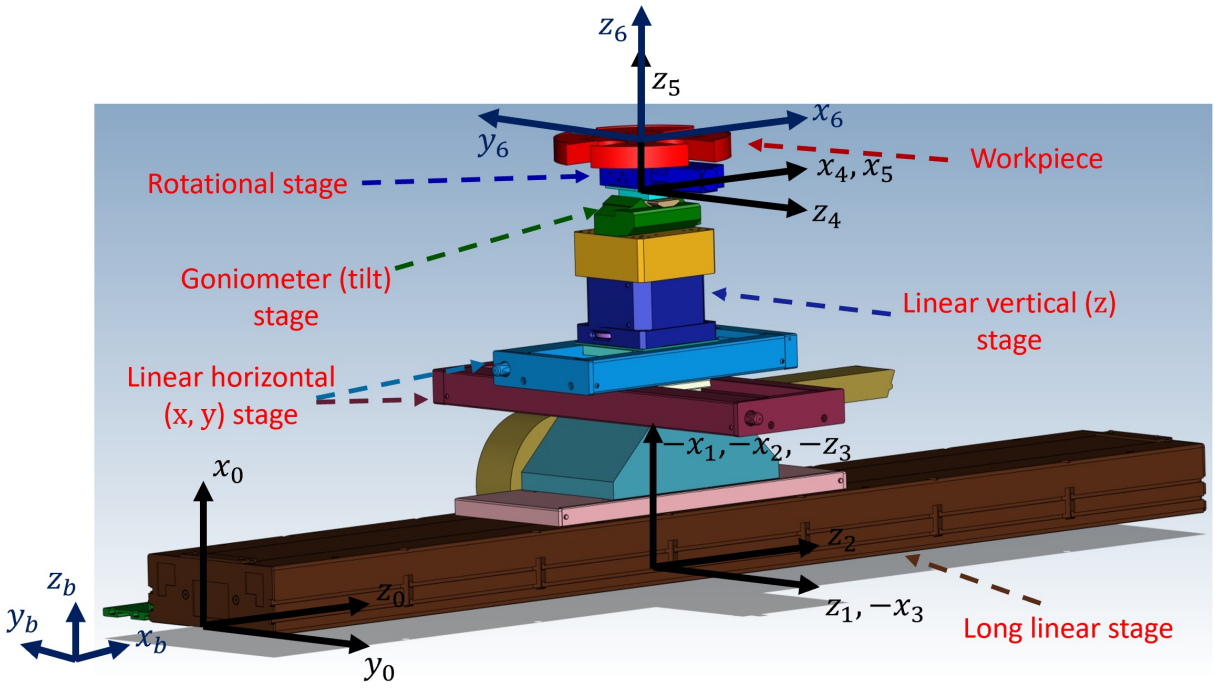

FIGURE 1: CAD MODEL AND COORDINATE FRAMES FOR THE PROPOSED POSITIONER ($\acute{P}P\acute{P}PR_tR_z$ ARRANGEMENT).

3D printing, and other advanced packaging capabilities for integrated microsystems such as microrobots and wearable sensors and actuators realized on flexible substrate. In its final configuration, this system will include two robots and three precision positioners, and additive process including deposition of multi-material features of 20 micron wide.

In general, the design of precision kinematic chains is based on the analysis of error propagation through the chain, which can be described using D-H parameters [5], product of exponentials [6], and interval analysis [7]. which are computationally intensive, and need additional mathematical formulation and programming. In this paper, we used kinematic sensitivity indices to study the error propagation [8, 9], which have a straightforward calculation approach, and also, provide intuitive physical meaning, as the calculation approach does not have summation of inconsistent units of translation and rotational DOFs.

The performance indices of robotic mechanisms have received much attention from the robotics research community [8], due to the need to provide comparisons between different robot architectures. The common indices are manipulability and dexterity of the mechanisms which entail some drawbacks regarding the summation of inconsistent units of rotational and translational degrees of freedom [8, 10–13]. In [8, 9], two distinct metrics are proposed: one for rotations of the mechanisms and one for their point-displacements. They are referred to as the kinematic sensitivity indices [8, 9].

In this paper, to study the error propagation of the positioner, a simple computational methodology is proposed which uses Jacobian of the mechanism, and is based on the kinematic sensitivity indices [8, 9]. Refinements have been made to the the computation methodology of these indices, and to the best of authors' knowledge, these indices have not been used before for study and design of precision positioners. The methodology facilitates quick modeling and analysis of different positioners. The analytical and computational nature of the methodology makes the method suitable to be used with optimization algorithms for optimal design of precision robots.

METHODS

To design our positioner, we checked the possibility of assembling individual stages, and using serial robotic arms or parallel mechanisms. The available serial robotic arms with payload requirements of our application are bulky, and they have a poor performance in terms of repeatability. The parallel mechanisms are well-known for having lower repeatability and high payloads [15]. However, the workspace of these mechanisms is typically limited, and larger mechanisms should be used for a given workspace. As a direct consequence, proper mechanisms are bulky and significantly more expensive.

Hence, assembling of individual precision stages was one of the few viable solutions for our application. In selection of the stages for the positioner, there were multiple conditions that needed to be met while maintaining a reasonable price range for

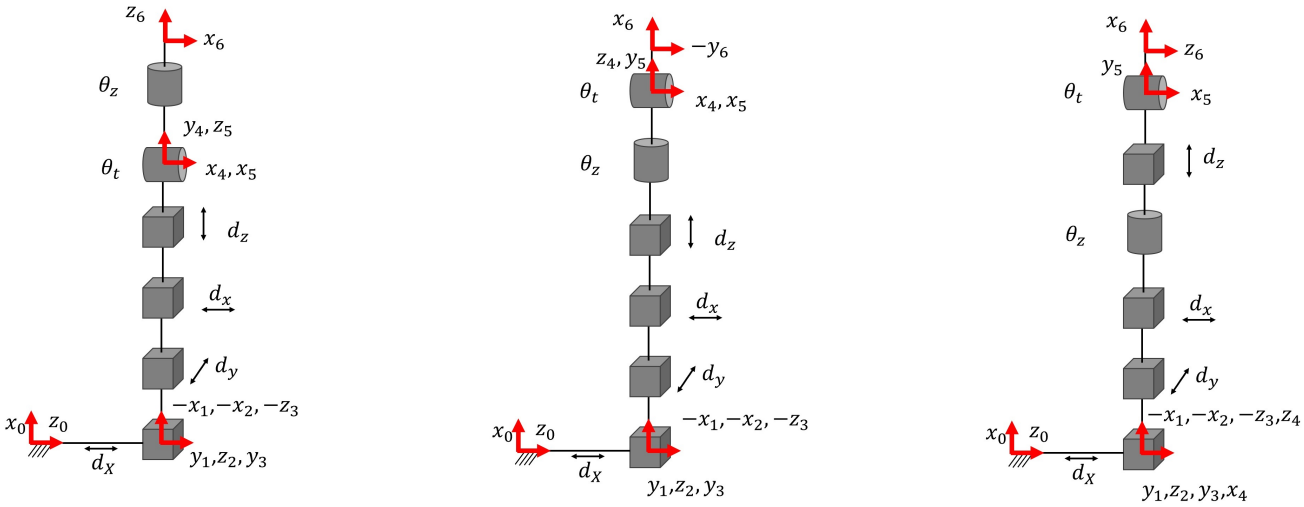

$\acute{P}P\acute{P}PR_tR_z$ $\acute{P}P\acute{P}PR_zR_t$ $\acute{P}P\acute{P}R_zPR_t$

FIGURE 2: COORDINATE FRAME ASSIGNMENT TO THE THREE DIFFERENT ARRANGEMENTS BASED ON DENAVIT-HARTENBERG CONVENTION [14].

the stages, including weight of the stages, maximum load of the stages, and height of each stage.

A versatile 6-DOF mechanism can be used for complete control of positioning and orientation of the workpiece. However, considering the required motion patterns in our application, we decided to eliminate one of the rotational degrees of freedom by removing one of goniometric stages. Hence, the developed mechanism had 5-DOF, for x-y-z linear motions, a continuous (360 deg) rotation along z axis (normal to ground), and a goniometric (tilt) stage (Fig. 1).

The positioner was required to move between multiple stations, and so, the positioner needed to have a large workspace in one direction (it is named x direction here, Fig. 1). However, long linear stages with low repeatability are usually expensive. Hence, we decided to use two linear stages to meet our workspace and repeatability requirements, one with large stroke for coarse motion of the positioner, and another one for fine adjustment of the positioner along x direction.

For our application the maximum load of 2kg needed to be carried by the positioner. Also, the weight of upper stages needed to be carried by the lower stages. Furthermore, metal adapters (buckets) were used to connect the stages together (to reduce the mechanism's error due to compression/extension and bending forces/torques), and weight of these adapters needed to be carried by the stages.

Additionally, height of the positioner could not exceed 50cm, as the positioner is needed to move between different stations. After reviewing the weight, height, and cost limitations, we decided to utilize the stages with specifications presented in Tab. 1. The stages were selected from catalogs of available stages from various manufacturers, including Newport Corporation, Intelligent Actuator Inc., and Physik Instrumente L.P. (CAD models of the selected stages were used to prepare the assembly model shown in Fig. 1).

For the required motion pattern, we had the following order of stages[1] (Fig. 2):

TABLE 1: SPECIFICATIONS OF THE STAGES. THE REPEATABILTY VALUES ARE BIDIRECTIONAL ($\pm$) AND PRESENTED IN MICROMETER (μm) AND MILLIDEGREE ($mdeg$) FOR LINEAR AND ROTATIONAL STAGES, RESPECTIVELY.

Stage	long x	y	x	z	θ_t	θ_z
Repeatability	3	0.15	0.15	0.1	6.5	2
Travel (mm, deg)	2300	300	100	30	$\pm$30	$\pm$180
Height (mm)	95	40	40	130	57.5	30
Payload (kg)	45	15	15	4	10	2
Weight (kg)	50	8.9	6.5	3	0.8	0.7

[1]The letters P and R represent linear and rotational degrees of freedom (taken from prismatic and revolute joint types). The ´ is used to show the stages with parallel axis of motion. The subtitles $_t$ and $_z$ represent the rotational and tilt degrees of freedom.

TABLE 2: D-H PARAMETERS FOR THE ŔPṔPR$_t$R$_z$, ŔPṔPR$_z$R$_t$ AND ŔPṔR$_z$PR$_t$ CONFIGURATIONS. MAJORITY OF THE PARAMETERS ARE IDENTICAL. THE NONIDENTICAL PARAMETERS ARE SEPARATED USING | SYMBOL.

Link	a$_i$	α_i	d$_i$	θ_i
1	0	$\frac{\pi}{2}$	d$_X$	π
2	0	$\frac{3\pi}{2}$	d$_y$	0
3	0	$\frac{\pi}{2}$	d$_x$	$\frac{\pi}{2}$
4	0	π	$-(l_1+d_z)$ | $-(l_1+d_z)$ |0	$\frac{\pi}{2}$ | $\frac{\pi}{2}$ | $(\frac{\pi}{2}+\theta_z)$
5	0	$\frac{3\pi}{2}$ | $\frac{\pi}{2}$ | $\frac{\pi}{2}$	0 | 0 |(l$_1$+d$_z$)	$-\theta_t$ | 0 | 0
6	0 | $-l_2$ | $-l_2$	0 | 0 | $\frac{\pi}{2}$	l_2 | 0 | 0	$-\theta_z$ | $\frac{\pi}{2}+\theta_t$ | $\frac{\pi}{2}+\theta_t$

ŔPṔPR$_t$R$_z$: a decoupled order of linear and rotational stages were assembled together with the linear stages close to the mechanism base, and continuous rotational stage at top.
ŔPṔPR$_z$R$_t$: the same decoupled order of linear and rotational stages with an inverse order of goniometer and rotational stages.
ŔPṔR$_z$PR$_t$: a coupled order of linear and rotational stages, with the z linear stage between the two rotational stages.

Selection of each stage order would result in a different repeatability for the final positioner. In rest of the paper, we present details of error propagation analysis for the ŔPṔPR$_t$R$_z$ structure, and the results for the two other configurations will be summarized in a table. It is noteworthy that the order of linear stages did not change the positioner's repeatability, as they generate decoupled motion in x, y and z directions.

Mechanism Kinematics and Jacobian

This section is devoted to the kinematic and Jacobian analysis of the positioner. The analysis is required for computation of error propagation along the mechanism's kinematic chain. Error of the positioner's end-effector is a compound error resulting from the translational and rotational errors of its individual stages. In order to extract the forward kinematic and Jacobian equations of the mechanism using D-H convention [14], proper coordinate frames were assigned to each positioner's joint (stage), and D-H parameters were obtained (Fig. 1). Table 2 tabulates the parameters.

To obtain forward kinematics, transformation matrices of different joints were obtained. Then transformation matrices were multiplied together. Eventually, the position (**d**) and orientation ($^6R_0$) of the end-effector were obtained from the final transformation matrix as follows:

$$\mathbf{d} = \begin{bmatrix} d_z + l_1 + l_2\cos(\theta_t) \\ d_y \\ d_X + d_x - l_2\sin(\theta_t) \end{bmatrix}, \tag{1}$$

$$^0R_6 = \begin{bmatrix} -\cos(\theta_z)\sin(\theta_t) & \sin(\theta_z)\sin(\theta_t) & -\cos(\theta_t) \\ \sin(\theta_z) & \cos(\theta_z) & 0 \\ \cos(\theta_z)\cos(\theta_t) & -\sin(\theta_z)\cos(\theta_t) & -\sin(\theta_t) \end{bmatrix}. \tag{2}$$

Clearly, the position of the end-effector is a function of variables of all the stages (d_X, d_y, d_x, d_z, θ_t, and θ_z), and hence, the translational error of the end-effector is expected to be a function of all the variables. However, the orientation of the end-effector (Eqn. (2)) is only a function of θ_t and θ_z, and consequently, the orientation error of the positioner is a pure function of its two rotational stages.

The vector **d** and the matrix $^6R_0$ are in $x_0y_0z_0$ coordinates. To have them in $x_by_bz_b$, pre-multiply them with the following rotation matrix:

$$^bR_0 = \begin{bmatrix} 0 & 0 & 1 \\ 0 & -1 & 0 \\ 1 & 0 & 0 \end{bmatrix}. \tag{3}$$

Jacobian shows the relationship between infinite small motion in joint space and workspace. Using conventional D-H methodology, the positioner's Jacobian was obtained as follows:

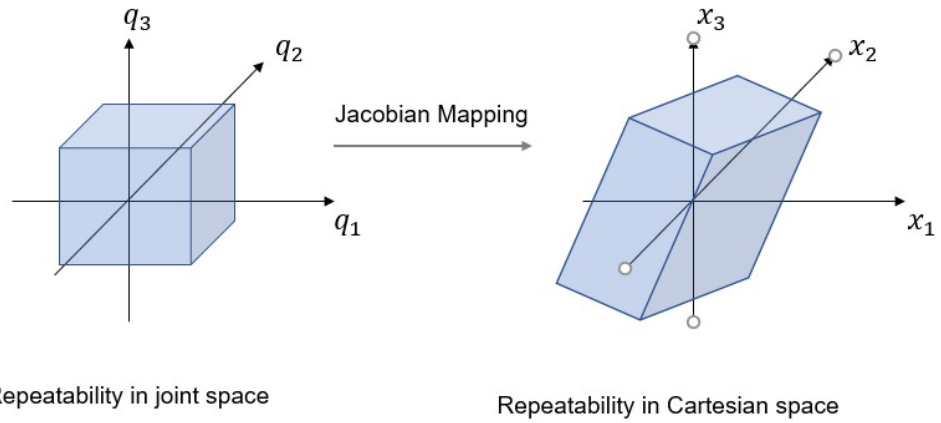

FIGURE 3: PROPAGATION OF MECHANISM REPEATABILITY FROM JOINT SPACE TO CARTESIAN SPACE. q_i (i=1,...,n) AND x_j (j=1,...,m) ARE JOINT SPACE AND CARTESIAN SPACE VARIABLES (n=6, m=5).

$$J = \begin{bmatrix} J_v \\ J_\omega \end{bmatrix} = \begin{bmatrix} 0\ 0\ 0\ 1 & -l_2\sin(\theta_t) & 0 \\ 0\ 1\ 0\ 0 & 0 & 0 \\ 1\ 0\ 1\ 0 & -l_2\cos(\theta_t) & 0 \\ 0\ 0\ 0\ 0 & 0 & cos(\theta_t) \\ 0\ 0\ 0\ 0 & -1 & 0 \\ 0\ 0\ 0\ 0 & 0 & -\sin(\theta_t) \end{bmatrix}. \quad (4)$$

Note that the Jacobian matrix J has two partitions (J_ω and J_v) corresponding to the angular and linear velocities of the end-effector. J_ω and J_v are used to obtain the maximum orientation and maximum translation errors of the end-effector, respectively.

Error Propagation Formulation

To formulate the positioner's error propagation, kinematic sensitivity indices were utilized in this paper. Kinematic sensitivity of mechanisms was introduced in [8] as performance indices for comparison and optimization of mechanical structures. These kinematic sensitivity indices provide tight upper bounds to the magnitudes of the end-effector rotations and point-displacements, respectively, under a *unit-magnitude* array of actuated-joint displacements. Maximum end-effector rotations (σ_r), and point-displacement (σ_p) can be defined as:

$$\sigma_r = \max_{||\rho||_\infty \leq 1} ||\phi||_2, \quad (5)$$

$$\sigma_p = \max_{||\rho||_\infty \leq 1} ||\mathbf{p}||_2, \quad (6)$$

where ϕ is the array of small rotations of the end-effector about the Cartesian axes, $\mathbf{p}$ represents a small displacement of the operation point, and ρ is the array of small actuator displacements which can be considered as the errors of the actuators. These two indices are referred to as the maximum orientation and point-displacement sensitivities, respectively [8].

In this paper, with some modifications, we used the same kinematic sensitivity indices for computation of error propagation. Specifically, kinematic sensitivity indices are error amplification factors of mechanisms. However, in this paper, we compute error of the mechanism (positioner) due to the repeatability of stages. To clarify, the stages we have used to build our positioner have different expected maximum error (repeatability). Hence, instead of finding the kinematic sensitivity due to the unit-magnitude array of joint motion, we calculate the maximum error (repeatability) of the end-effector as a result of the repeatability of stages [9].

Jacobian shows the relation between infinite small motion in joint space and workspace. The bounded error in joint space can be represented by a hypercube[2] (Fig. 3). The hypercube is mapped to a polyhedron in Cartesian space[3]. The polyhedron in Cartesian space is convex, and so, the maximum error corresponds with Euclidean norm of one of the vertices of the polyhedron. The vertices of the polyhedron in joint space is obtained through multiplication of the mechanism's Jacobian to the vertices of the hypercube in joint space. To find the maximum rotational and translational error (σ_r and σ_p, respectively), the Euclidean norm ($||.||_2$) of the polyhedron's vertices should be calculated and compared with each other [9].

Differential kinematics of the mechanism is written as be-

[2]The hyper cube in this paper is in a 6D space (n=6) as the positioner is built by six stages.

[3]The polyhedron is in a 5D space (m=5) as the positioner has 5 degrees of freedom.

low:

$$\dot{x} = \begin{bmatrix} \dot{x} \\ \dot{y} \\ \dot{z} \\ \dot{\phi}_x \\ \dot{\phi}_y \\ \dot{\phi}_z \end{bmatrix} = J\dot{q} = \begin{bmatrix} J_v \\ J_\omega \end{bmatrix} q. \tag{7}$$

In order to find the linear and angular velocities of the end-effector separately, the differential kinematics of the mechanism can be re-written as following:

$$\begin{bmatrix} \dot{x} \\ \dot{y} \\ \dot{z} \end{bmatrix} = J_v\dot{q}, \qquad \begin{bmatrix} \dot{\phi}_x \\ \dot{\phi}_y \\ \dot{\phi}_z \end{bmatrix} = J_\omega\dot{q}. \tag{8}$$

Using Eqn. 8, we can find the vertices of the polyhedron mapped from the vertices of the hypercube in joint space. Repeatability of stages in joint space constitutes the vertices of hypercube (plus and minus values of repeatability values are vertices in different quadrants). The maximum end-effector rotation and point-displacement can be obtained using the equations below:

$$\sigma_r = \max_{i=1,\dots,n} \sqrt{\phi_x^2 + \phi_y^2 + \phi_z^2},$$

$$\sigma_p = \max_{i=1,\dots,n} \sqrt{x_i^2 + y_i^2 + z_i^2}, \tag{9}$$

where n is the number of vertices.

Sensitivity of mechanisms varies at different points of the workspace, and so, the kinematic sensitivity indices are local performance measures. To clarify, these indices are obtained using the mechanism's Jacobian, and Jacobian matrrix varies at different points in workspace. Hence, to find the maximum possible error of the mechanism, the mechanism's workspace should be searched to find the maximum σ_r and σ_p values. Previously, interval analysis [16] and Monte Carlo simulation [17] methods have been used for this purpose. However, due to the simple structure of the positioner, we utilize the 'fsolve' function of MATLAB® to search the workspace and to find the maximum values of σ_p and σ_r.

RESULTS

Specifications of the stages used in this project are tabulated in Tab. 1. Vertices of the repeatability hypercube in joint space are obtained considering positive or negative ($\pm$) repeatability values:

$$V = 10^{-6} \times [\pm 3, \pm 0.15, \pm 0.15, \pm 0.1, \pm 113, \pm 35]^T. \tag{10}$$

Equations (8) and (9) are used to calculate repeatability of the end-effector in different scenarios. Several sets of Cartesian space errors are introduced in this section.

The coarse or fine linear x–stages can be used to implement the motion patterns, and as they have different repeatability, they will result in different workspace errors. The error for implementation of motion patterns with coarse long linear stage is

$$\sigma_r = 6.8\ mdeg, \qquad \sigma_p = 9.78\ \mu m. \tag{11}$$

The error for implementing the motion patterns with fine linear stage is

$$\sigma_r = 6.8\ mdeg, \qquad \sigma_p = 6.96\ \mu m. \tag{12}$$

In addition to the cases of using the entire positioner, three additional scenarios were considered here.

(1) Implementing a motion solely using the linear stages (assuming that we can perfectly determine the initial orientation of the rotational stages):

with coarse long linear stage along x:

$$\sigma_r = 0\ mdeg, \qquad \sigma_p = 3.01\ \mu m, \tag{13}$$

and with fine linear stage along x:

$$\sigma_r = 0\ mdeg, \qquad \sigma_p = 0.23\ \mu m. \tag{14}$$

(2) Implementing a motion solely using the rotational stages (assuming that we can perfectly determine the initial location of the linear stages):

$$\sigma_r = 6.8\ mdeg, \qquad \sigma_p = 6.78\ \mu m. \tag{15}$$

(3) Implementing a motion solely using the goniometric (tilt) stage:

$$\sigma_r = 6.5\ mdeg, \qquad \sigma_p = 6.78\ \mu m. \tag{16}$$

Table 3 summarizes the maximum rotational and translational for the three different arrangement of the stages.

TABLE 3: ERROR RELATED TO DIFFERENT ARRANGEMENTS OF STAGES. TRANSLATIONAL ERROR AND ROTATIONAL ERROR ARE PRESENTED IN MICRON (μm) AND MILLIDEGREE ($mdeg$), RESPECTIVELY.

Stages		$\acute{P}P\acute{P}PR_tR_z$	$\acute{P}P\acute{P}PR_zR_t$	$\acute{P}P\acute{P}R_zPR_t$
All	long x	$\sigma_r = 6.8$ $\sigma_p = 9.78$	$\sigma_r = 6.8$ $\sigma_p = 10.04$	$\sigma_r = 6.8$ $\sigma_p = 9.78$
	fine x	$\sigma_r = 6.8$ $\sigma_p = 6.96$	$\sigma_r = 6.8$ $\sigma_p = 7.29$	$\sigma_r = 6.8$ $\sigma_p = 7.29$
Translational	long x	$\sigma_r = 0$ $\sigma_p = 3.01$	$\sigma_r = 0$ $\sigma_p = 3.01$	$\sigma_r = 0$ $\sigma_p = 3.01$
	fine x	$\sigma_r = 0$ $\sigma_p = 0.23$	$\sigma_r = 0$ $\sigma_p = 0.23$	$\sigma_r = 0$ $\sigma_p = 0.23$
Rotational		$\sigma_r = 6.8$ $\sigma_p = 6.78$	$\sigma_r = 6.8$ $\sigma_p = 6.78$	$\sigma_r = 6.8$ $\sigma_p = 6.78$

DISCUSSION

The values computed in previous section are the maximum expected errors of the mechanism in its entire workspace (worst case scenario). Table 3 summarizes the results for the three arrangements. During the implementation of motion patterns using all the stages, the $\acute{P}P\acute{P}PR_tR_z$ arrangement has better repeatability performance than the $\acute{P}P\acute{P}PR_zR_t$ and $\acute{P}P\acute{P}R_zPR_t$ structures. However, when using only the linear stages or the rotational stages, errors of the mechanisms are identical.

As expected, using the fine linear stage results in a smaller translational error for implementation of motion patterns. However, using the coarse or fine linear stages does not change the maximum rotational error of the mechanism (σ_r).

The scenarios of using only rotational stages or translational stages for implementation of motion patterns, suggest that using fewer number of stages results in smaller error for the end-effector. As an intuitive result, if we intend to track a straight line, and the line is not (purely) along x or y directions (for example, line y=x, for which we need to use both x and y stages to implement the motion), then it is better to use the rotational stage (with rotation along z) to orient the workpiece in the proper direction and implement the motion with just one of the stages.

In this paper, we only considered the repeatability error of stages, and we assumed that the stages were connected without misalignment. This is a limitation of our work and in future work, we are going to include more sources of error in our calculations [18], [19]. It will result in a better estimation of the end-effector repeatability (error).

CONCLUSION

Error propagation analysis can be used as tool for estimating the performance of robotic mechanisms (in terms of end-effector's repeatability) before prototyping them. Hence, additive manufacturing can benefit hugely from this analysis, as the technology is highly dependent on the repeatability of their mechanical positioning and manipulation systems. In this paper, we presented a novel methodology for the study of error propagation in serial robotic chains. The methodology is based on kinematic sensitivity analysis of them mechanism using its Jacobian matrix. We applied the methodology to the analysis and design of a precision robotic 5-DOF positioner that we developed for application in precision robotics. The positioner was prepared through serial attachment of linear and rotational stages. Three different arrangements of stages were studied, and it was shown that different orders of stages results in different translation and orientation repeatability for the positioner. Our analyses and results support the use of our methodology as a tool for the the design and optimization of multi-DOF positioners.

In the future, we are going to include more sources of error (like misalignment of the stages) in our analyses for better estimation of the mechanism's precision. We are also planning to build the positioner for 3D printing in our Nexus system. We will use displacement sensors for experimental evaluation of the positioner and our computations.

ACKNOWLEDGMENT

This work was supported by National Science Foundation awards MRI #1828355, and EPSCOR #1849213. We wish to thank Antonie Blasiak, Aditya N. Das, Andriy Sherehiy and Danming Wei for their contributions to the positioner requirements within the Nexus system.

REFERENCES

[1] Donald, B. R., Levey, C. G., and Paprotny, I., 2008. "Planar microassembly by parallel actuation of mems microrobots". *Journal of Microelectromechanical Systems,* ***17***(4), pp. 789–808.

[2] Popa, D. O., and Stephanou, H. E., 2004. "Micro and mesoscale robotic assembly". *Journal of manufacturing processes,* ***6***(1), pp. 52–71.

[3] Das, A. N., Murthy, R., Popa, D. O., and Stephanou, H. E., 2011. "A multiscale assembly and packaging system for manufacturing of complex micro-nano devices". *IEEE Transactions on Automation Science and Engineering,* ***9***(1), pp. 160–170.

[4] King, B. H., and Ramahi, D. H., 2009. Aerosol jet (r) printing system for photovoltaic applications, Mar. 5. US Patent App. 12/203,074.

[5] Slocum, A. H., 1992. *Precision machine design*. Society of Manufacturing Engineers.

[6] Das, A. N., and Popa, D. O., 2011. "Precision evaluation of modular multiscale robots for peg-in-hole microassembly tasks". In 2011 IEEE/RSJ International Conference on Intelligent Robots and Systems, IEEE, pp. 1699–1704.

[7] Pac, M. R., and Popa, D. O., 2012. "Interval analysis for robot precision evaluation". In 2012 IEEE International Conference on Robotics and Automation, IEEE, pp. 1087–1092.

[8] Cardou, P., Bouchard, S., and Gosselin, C., 2010. "Kinematic-sensitivity indices for dimensionally nonhomogeneous jacobian matrices". *IEEE Transactions on Robotics,* ***26***(1), pp. 166–173.

[9] Saadatzi, M. H., Masouleh, M. T., Taghirad, H. D., Gosselin, C., and Cardou, P., 2011. "Geometric analysis of the kinematic sensitivity of planar parallel mechanisms". *Transactions of the Canadian Society for Mechanical Engineering,* ***35***(4), pp. 477–490.

[10] Yoshikawa, T., 1985. "Manipulability of robotic mechanisms". *The international journal of Robotics Research,* ***4***(2), pp. 3–9.

[11] Khan, W. A., and Angeles, J., 2005. "The Kinetostatic Optimization of Robotic Manipulators: The Inverse and the Direct Problems". *Journal of Mechanical Design,* ***128***(1), 08, pp. 168–178.

[12] Stocco, L. J., Salcudean, S. E., and Sassani, F., 1999. "On the use of scaling matrices for task-specific robot design". *IEEE Transactions on Robotics and Automation,* ***15***(5), pp. 958–965.

[13] Merlet, J. P., 2005. "Jacobian, Manipulability, Condition Number, and Accuracy of Parallel Robots". *Journal of Mechanical Design,* ***128***(1), 06, pp. 199–206.

[14] Spong, M. W., Hutchinson, S., Vidyasagar, M., et al., 2006. *Robot modeling and control*, Vol. 3. wiley New York.

[15] Briot, S., and Bonev, I. A., 2007. "Are parallel robots more accurate than serial robots?". *Transactions of the Canadian Society for Mechanical Engineering,* ***31***(4), pp. 445–455.

[16] Khalilpour, S., Loloei, A. Z., Masouleh, M. T., and Taghirad, H., 2013. "Kinematic performance indices analyzed on four planar cable robots via interval analysis". In 2013 First RSI/ISM International Conference on Robotics and Mechatronics (ICRoM), IEEE, pp. 313–318.

[17] Das, A. N., Zhang, P., Lee, W. H., Popa, D., and Stephanou, H., 2007. "μ^3: multiscale, deterministic micro-nano assembly system for construction of on-wafer microrobots". In Proceedings 2007 IEEE International Conference on Robotics and Automation, IEEE, pp. 461–466.

[18] Caro, S., Binaud, N., and Wenger, P., 2009. "Sensitivity analysis of 3-rpr planar parallel manipulators". *Journal of mechanical design,* ***131***(12).

[19] Kim, H. S., and Tsai, L.-W., 2003. "Design optimization of a cartesian parallel manipulator". *J. Mech. Des.,* ***125***(1), pp. 43–51.